

Spin glass-like behavior of Ge:Mn

C. Jaeger,^{*} C. Bihler, and T. Vallaitis[†]

Walter Schottky Institut, Technische Universität München

Am Coulombwall 3, 85748 Garching, Germany

S. T. B. Goennenwein, M. Opel, and R. Gross

Walther-Meissner-Institut, Bayerische Akademie der Wissenschaften

Walther-Meissner-Str. 8, 85748 Garching, Germany

M. S. Brandt

Walter Schottky Institut, Technische Universität München

Am Coulombwall 3, 85748 Garching, Germany

Abstract

We present a detailed study of the magnetic properties of low-temperature molecular beam epitaxy grown Ge:Mn dilute magnetic semiconductor films. We find strong indications for a spin glass-like behavior of Ge:Mn at low temperatures. For a $\text{Ge}_{0.96}\text{Mn}_{0.04}$ sample, the zero-field cooled magnetization is only about 40% of the field cooled magnetization below a freezing temperature $T_f = 12$ K. In addition, AC susceptibility measurements show a peak around T_f , with the peak position T'_f shifting as a function of the driving frequency f by $\Delta T'_f/[T'_f \cdot \Delta \log f] \approx 0.06$. Furthermore, we observe relaxation effects of the magnetization after switching the external magnetic field below T_f which are in qualitative agreement with the field and zero-field cooled magnetization measurements. These findings consistently show that Ge:Mn exhibits spin-glass like magnetic behavior at low temperatures, and that it is not a conventional ferromagnet.

PACS numbers: 75.50.Lk, 75.50.Pp, 75.70.-i, 76.60.Es

^{*}Electronic address: christian.jaeger@wsi.tum.de

[†]Present address: Universität Karlsruhe, Engesserstr. 5, 76131 Karlsruhe, Germany

I. INTRODUCTION

Diluted magnetic semiconductors (DMS) - obtained by doping semiconductor materials with magnetic impurities - have been investigated extensively due to their potential application in spintronic devices. In particular, the most prominent material system $\text{Ga}_{1-x}\text{Mn}_x\text{As}$ is generally assumed to exhibit a hole-mediated long-range ferromagnetic order with Curie temperatures of up to $T_C = 172$ K.[1, 2, 3] In contrast to conventional ferromagnetism, many DMS systems were found to exhibit spin glass state. As an example, the observation of a spin glass phase in Mn-doped II-VI DMSs like $\text{Zn}_{1-x}\text{Mn}_x\text{Te}$,[4] $\text{Cd}_{1-x}\text{Mn}_x\text{Te}$,[5, 6] and $\text{Cd}_{1-x}\text{Mn}_x\text{Se}$ ($x > 0.2$)[6] has been reported more than two decades ago. Recently, spin glass behavior was discovered for the III-V diluted magnetic semiconductors $\text{Ga}_{1-x}\text{Mn}_x\text{N}$ with a spin freezing temperature of $T_f = 4.5$ K ($x \approx 0.1$)[7] and Te-doped $\text{Ga}_{1-x}\text{Mn}_x\text{As}$ with $T_f = 30$ K ($x = 0.085$).[8]

As the first ferromagnetic group-IV DMS, Park *et al.* reported in 2002 the growth of $\text{Ge}_{1-x}\text{Mn}_x$ with T_C up to 116 K for $x = 0.033$. [9] The control of the hole densities in gated Hall bar samples allowed a switching of the ferromagnetic order, which was used as a proof of hole-mediated ferromagnetism in this material.[9] Cho *et al.* reported ferromagnetism with a $T_C = 285$ K in Mn-doped bulk single crystals,[10] but the magnetic properties of their samples were clearly dominated by the presence of the intermetallic compound $\text{Mn}_{11}\text{Ge}_8$. [11, 12] These reports of high- T_C ferromagnetism in $\text{Ge}_{1-x}\text{Mn}_x$ are in contrast to recent findings of Li *et al.*, [13, 14] who propose to use two ordering temperatures (T_C^* and T_C) to describe the magnetic coupling in Ge:Mn. Here, the higher transition temperature T_C^* refers to the onset of local ferromagnetism, whereas only at a much lower transition temperature T_C a percolation transition leading to global ferromagnetism takes place. The values found for T_C for a sample with 5 at.% Mn are of the order of 10 K, which indicates that $\text{Ge}_{1-x}\text{Mn}_x$ is far away from being a high- T_C DMS. Also, scanning photoelectron microscopy analysis by Kang *et al.* indicates that ferromagnetism in Mn-doped Ge is not of intrinsic nature,[12] but arises from magnetic properties of Mn-rich clusters in phase-segregated $\text{Ge}_{1-x}\text{Mn}_x$.

In this work, we present a detailed study of the magnetic properties of low-temperature molecular beam epitaxy (LT-MBE) grown Ge:Mn films. Magnetization measurements for different cooling fields, a frequency dependent shift of the AC susceptibility peak, and relaxation effects in time-dependent magnetization measurements are strong indications for the

presence of a frozen state in $\text{Ge}_{1-x}\text{Mn}_x$ at low temperatures. These findings suggest a more complex magnetic behavior of Ge:Mn, rather than conventional ferromagnetism.

II. EXPERIMENTAL DETAILS

The Ge:Mn samples studied were grown on semi-insulating Ge(100) substrates via LT-MBE. Prior to the deposition process, the substrates were heated to 600°C for 30 minutes in the MBE system to evaporate the oxide layer. The flux from the Mn effusion cell was calibrated by elastic recoil detection (ERD) analysis and energy dispersive x-ray (EDX) measurements. We investigated growth at different substrate temperatures ($110^\circ\text{C} \leq T_S \leq 225^\circ\text{C}$) and growth rates ($0.1 \text{ \AA/s} \leq R_{\text{Ge}} \leq 1 \text{ \AA/s}$) and discuss the magnetic properties of two samples in detail in this work characteristic for two different ranges of Mn concentration with a composition of $\text{Ge}_{0.96}\text{Mn}_{0.04}$ ($T_S = 150^\circ\text{C}$, $R_{\text{Ge}} = 0.3 \text{ \AA/s}$) and $\text{Ge}_{0.8}\text{Mn}_{0.2}$ ($T_S = 225^\circ\text{C}$, $R_{\text{Ge}} = 1 \text{ \AA/s}$).

All magnetization measurements were performed using a superconducting quantum interference device (SQUID) magnetometer. The temperature dependence of magnetization $M(T)$ was measured between 2 K and 330 K warming-up the sample in a constant external magnetic field $\mu_0 H_m = 1 \text{ mT}$ (indicated by solid symbols in the figures below) and $\mu_0 H_m = 100 \text{ mT}$ (open symbols). All fields were applied in the film plane. To investigate the influence of the thermal history of the samples on the measured magnetization curves, we applied different cooling procedures. In the following, cooling the sample in the maximal available magnetic field of $\mu_0 H_C = 7 \text{ T}$ is called maximum field cooling (MFC), whereas cooling without any applied magnetic field (nominal $\mu_0 H_C = 0 \text{ T}$) is denoted as zero-field cooling (ZFC). For the field cooled (FC) measurement, the measuring field is identical to the field applied during cooling the sample.

III. RESULTS AND DISCUSSION

A. Sample $\text{Ge}_{0.96}\text{Mn}_{0.04}$

Figure 1 shows the temperature dependence of the magnetization of the $\text{Ge}_{0.96}\text{Mn}_{0.04}$ sample. All magnetization measurements clearly show the presence of the intermetallic phase Mn_5Ge_3 , which contributes a ferromagnetic signal with a Curie temperature of

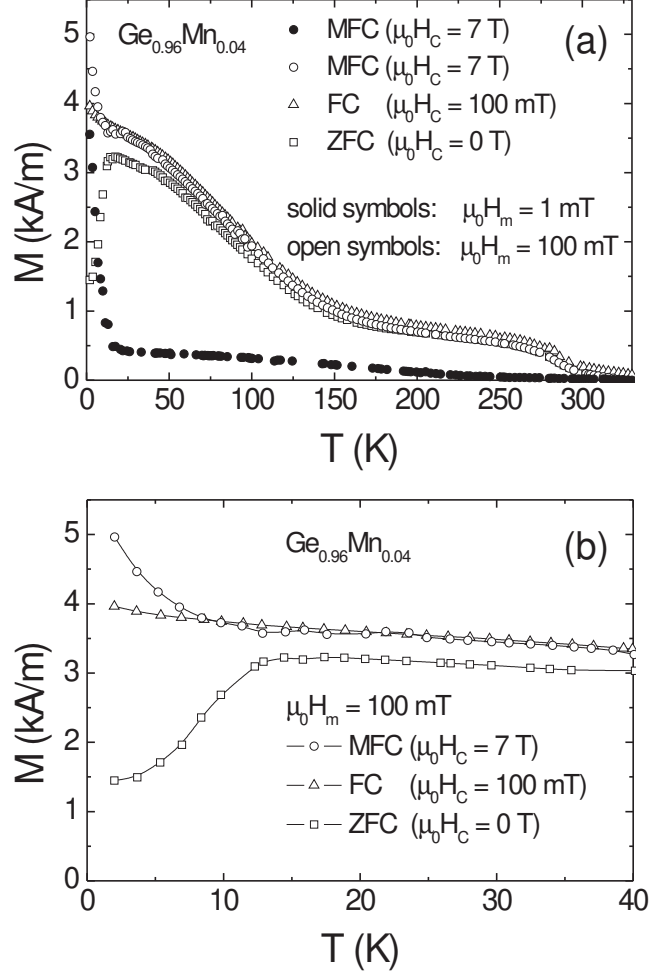


FIG. 1: (a) Temperature dependence of the magnetization of the $\text{Ge}_{0.96}\text{Mn}_{0.04}$ sample. The measurements were performed at $\mu_0 H_m = 1$ mT (solid symbols) and $\mu_0 H_m = 100$ mT (open symbols). The sample was cooled down in the maximal external magnetic field (MFC, $\mu_0 H_C = 7$ T), in zero magnetic field (ZFC) and in a field identical to the measuring field (FC). (b) Magnification of the low temperature regime of the measurements with $\mu_0 H_m = 100$ mT in (a).

$T_C = 296$ K.[15] In our samples with $x \approx 0.03$ the Mn_5Ge_3 precipitates are preferentially incorporated with their easy magnetic [1000] axis aligned parallel to the [100] growth direction.[16] This explains the much weaker Mn_5Ge_3 -signal of the measurement in the smaller external magnetic field $\mu_0 H_m = 1$ mT aligned along the magnetic hard in-plane direction (solid symbols).

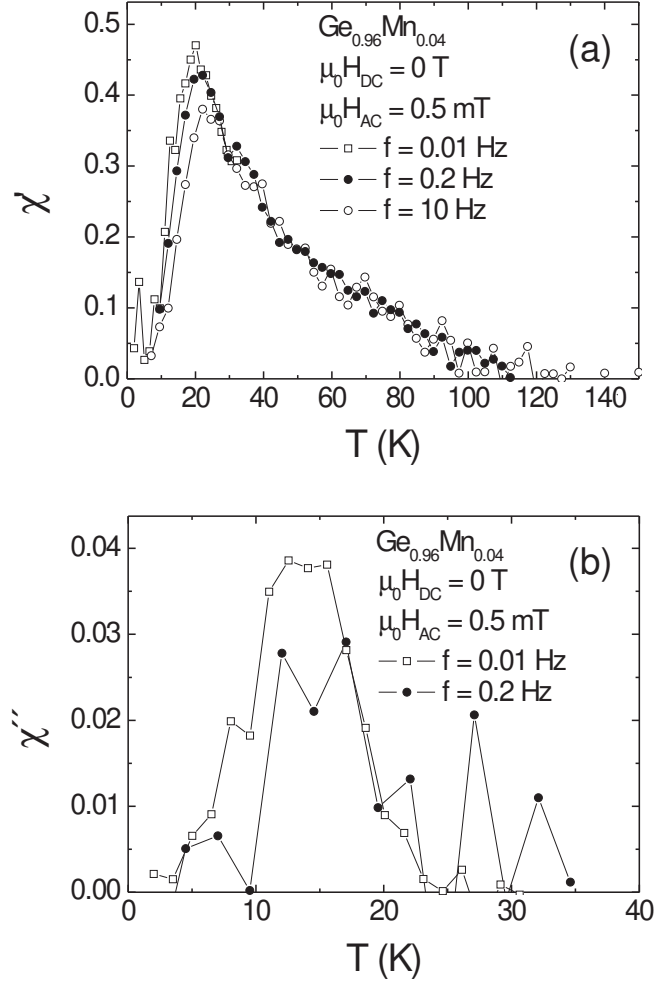


FIG. 2: (a) Real part $\chi'(T)$ of the AC susceptibility of the $\text{Ge}_{0.96}\text{Mn}_{0.04}$ sample. The measurement was performed with $\mu_0 H_{DC} = 0$ T and $\mu_0 H_{AC} = 0.5$ mT at different driving frequencies $f = 0.01$ Hz (open squares), $f = 0.2$ Hz (solid circles), and $f = 10$ Hz (open circles). (b) Imaginary part $\chi''(T)$ of the AC susceptibility.

In the MFC measurement with $\mu_0 H_m = 1$ mT, we observe a steep decrease of the magnetization for increasing temperatures below 15 K. For the MFC measurement at higher $\mu_0 H_m = 100$ mT, the dominant feature is a concave shoulder below ≈ 150 K in the $M(T)$ diagram, with a small additional decrease of $M(T)$ below 15 K. The fact that the shoulder only appears in the measurement with the higher magnetic field indicates superparamagnetic behavior in this temperature range. Li *et al.* [13, 14] explained similar magnetization vs. temperature curves via the picture of percolating bound magnetic polarons (BMPs) [17, 18].

From a Curie-Weiss plot of measurements performed at 100 mT, they deduce a temperature T_C^* , at which the BMPs start forming, while they assign T_C to the end of the steep decrease in $M(T)$ at lower temperatures. Applying the same analysis to our measurements, we obtain transition temperatures of $T_C = 17$ K and $T_C^* = 83$ K for $\text{Ge}_{0.96}\text{Mn}_{0.04}$, in good agreement with the values obtained by Li *et al.* [13, 14]

In addition, we performed FC (open triangles) and ZFC (open squares) measurements in an external magnetic field of $\mu_0 H_m = 100$ mT. Above 15 K, the magnetization curves show the same qualitative behavior as the MFC measurement at $\mu_0 H_m = 100$ mT. However, below 12 K, the FC and ZFC curves differ strongly from each other: whereas the FC magnetization decreases very little with increasing temperature, the ZFC curve starting from a lower magnetization at $T = 2$ K exhibits a strong increase of the magnetization (Fig. 1(b)). As the magnetization of this low-temperature state strongly depends on the history of the sample, this FC-ZFC difference is often interpreted as a fingerprint of spin glass systems.[7, 19] Here, it is important to note that the nucleation and growth of magnetic domains might cause similar effects in ferromagnetic materials. Nevertheless, further indications for the presence of a frozen state at low temperatures are provided by measurements of the AC susceptibility and the time-dependence of the magnetization discussed below. Therefore, we determine a freezing temperature $T_f = 12$ K for this sample from the onset of the strong difference between the FC and the ZFC measurements.

To learn more about the low-temperature state and its phase transition, frequency-dependent AC susceptibility measurements were performed. The results are shown in Fig. 2, with $\mu_0 H_{DC} = 0$ T and $\mu_0 H_{AC} = 0.5$ mT at $f = 0.01$ Hz (open squares), $f = 0.2$ Hz (solid circles) and $f = 10$ Hz (open circles). In the real part of the AC susceptibility χ' (Fig. 2(a)), a pronounced peak is visible for all three frequencies, accompanied by a monotonic decrease of the susceptibility to $\chi' = 0$ above 120 K. This is the temperature range where the concave shoulder is observed in the magnetization measurements at $\mu_0 H_m = 100$ mT. The imaginary part of the susceptibility $\chi''(T)$ (Fig. 2(b)) is about a tenth of the real part $\chi'(T)$, which leads to a reduced signal-to-noise ratio due to small sample volume. Nevertheless, a peak of $\chi''(T)$ can be observed for $f = 0.01$ Hz (open squares) and $f = 0.2$ Hz (solid circles).

A careful investigation of $\chi'(T)$ reveals a small shift of the peak position to higher temperatures for higher driving frequencies (Fig. 3). The peak positions are denoted with arrows, the smooth solid lines are guides to the eye. The intensity of the peak increases for lower mea-

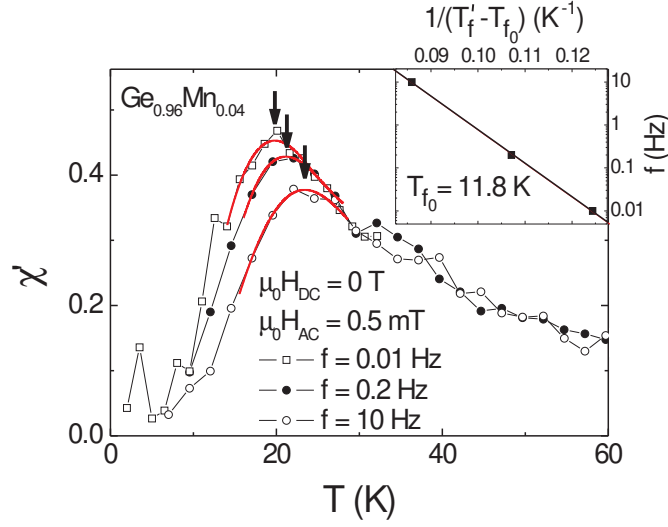


FIG. 3: (Color online) Real part $\chi'(T)$ of the AC susceptibility of the $\text{Ge}_{0.96}\text{Mn}_{0.04}$ sample in the vicinity of the peak positions. The notation is the same as in Fig. 2. The peak positions T'_f are indicated by arrows, the smooth solid lines are guides to the eye. The inset shows the dependence of the peak position temperatures T'_f (solid squares) on the measuring frequency f fitted with the Vogel-Fulcher law (straight line).

suring frequencies. Furthermore, $\chi'(T)$ curves for different measuring frequencies overlap for temperatures higher than the peak temperature. Such a behavior is observed in many spin glass systems and is usually taken as a clear indication for spin glass behavior [7, 20, 21, 22].

A quantitative measure of the frequency shift of the peak position is given by the relative shift of the peak temperature $\Delta T'_f/T'_f$ per decade shift in frequency. For the sample studied here, $\Delta T'_f/[T'_f \cdot \Delta \log f] \approx 0.06$, which is in agreement with values obtained for other spin glass systems, like 0.02 for $\text{Cd}_{0.6}\text{Mn}_{0.4}\text{Te}$, [23] 0.05 for $\text{Eu}_{0.6}\text{Sr}_{0.4}\text{S}$, [23] and 0.012 for $\text{Ga}_{1-x}\text{Mn}_x\text{N}$, [7] and smaller than the ≈ 0.3 expected for a superparamagnet, like 0.28 for $\alpha\text{-(Ho}_2\text{O}_3\text{)(B}_2\text{O}_3\text{)}$. [24]

Furthermore, the frequency dependence of the peak position of spin glasses can be described using the Vogel-Fulcher law [25]

$$f = f_0 \cdot \exp \left[-\frac{E_A}{k_B(T'_f - T_{f0})} \right], \quad (1)$$

with a activation energy E_A and a characteristic frequency f_0 . Here, T_{f0} has been interpreted

to take into account inter-cluster couplings [26]. It can be regarded as the true critical temperature for $f \rightarrow 0$, while T'_f , being higher than T_{f_0} , is the dynamic manifestation of the underlying phase transition [24]. The fit to the three peak positions for the $\text{Ge}_{0.96}\text{Mn}_{0.04}$ sample is shown in the inset of Fig. 3 with fit parameters of $E_A/k_B = 180$ K, $T_{f_0} = 11.8$ K and $f_0 = 5 \times 10^7$ Hz. $T_{f_0} = 11.8$ K is in agreement with the freezing temperature $T_f = 12$ K determined above from the difference between the FC and ZFC magnetization measurements. The E_A/k_B values are in the same range as observed for other glassy systems, like 108 K for $\text{Fe}_{1/3}\text{TiS}_2$ with $T_{f_0} = 48.7$ K [27] and 220 K for $\text{Co}_{0.2}\text{Zn}_{0.8}\text{Fe}_{1.6}\text{Ti}_{0.4}\text{O}_4$ with $T_{f_0} = 106$ K.[28] The obtained frequency f_0 is of the same order as the observed $f_0 \approx 10^7$ Hz for $\text{Co}_{0.2}\text{Zn}_{0.8}\text{Fe}_{1.6}\text{Ti}_{0.4}\text{O}_4$ [28] and $f_0 = 2.5 \times 10^7$ Hz for CuMn (with 4.6 at.% of Mn).[24]

To further elucidate the dynamics of the system, we also performed time-dependent magnetization measurements, using two different measurement procedures displayed schematically in the upper panels of Fig. 4.

In the first procedure (Fig. 4(a)), the sample was cooled from room temperature to a constant measurement temperature with no external magnetic field applied to the sample (ZFC). After the measurement temperature was stable, the external magnetic field was increased to $\mu_0 H = 100$ mT at a time denoted by t_1 in Fig. 4(a). After two hours of measurement denoted by t_2 in Fig. 4(a), the magnetic field was switched off again. We repeated this procedure for different measurement temperatures of 2 K, 5 K, 10 K, 15 K, and 40 K.

In the second procedure (Fig. 4(b)), the sample was cooled from room temperature to a constant measurement temperature with the maximum field $\mu_0 H_C = 7$ T applied to the sample (MFC). Then, we reduced the magnetic field, reaching 100 mT at a time t_3 . This procedure we again performed at different measurement temperatures of 2 K, 5 K, 10 K, 15 K, and 40 K. In the following, the time-dependent magnetization during the time interval $t_1 < t < t_2$ (Fig. 4(a)) will be denoted as $M_1(t)$. Likewise, $M_2(t)$ corresponds to $t > t_2$ (Fig. 4(a)), and $M_3(t)$ describes the results for $t > t_3$ of experiments following the second procedure (Fig. 4(b)).

A schematic illustration of the measured time dependence of the magnetization is shown in the lower panels of Fig. 4. For the ZFC procedure (Fig. 4(a)), the net magnetization in the sample after cooling down is zero. After the magnetic field is switched to $\mu_0 H = 100$ mT at t_1 , the magnetization jumps to a finite value $M_1^0 - M_1^r$, followed by an additional slow

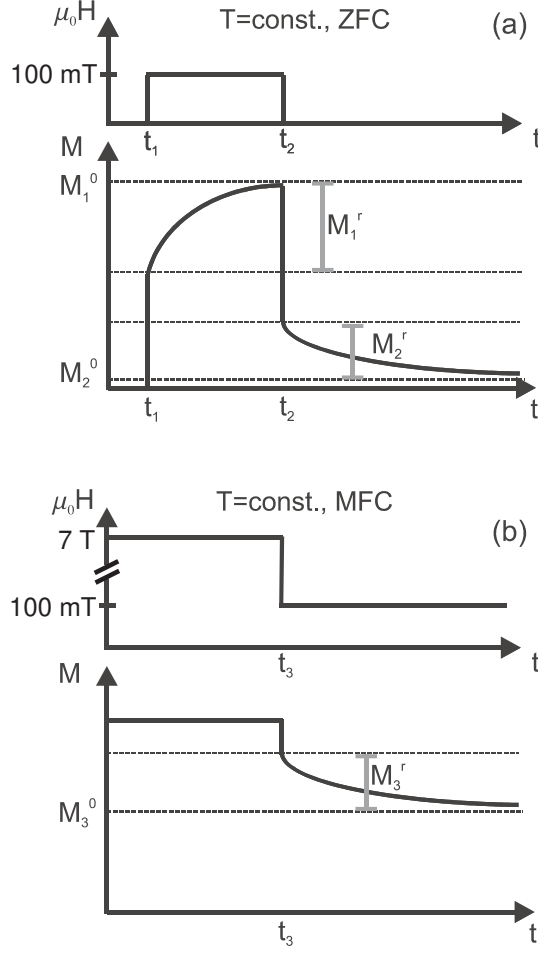


FIG. 4: Switching procedures of the external magnetic field (upper panels) for the time-dependent magnetization measurements shown schematically in the lower panels for (a) ZFC and (b) MFC.

increase to M_1^0 . After the magnetic field is switched off again at t_2 , the magnetization again jumps to a finite value $M_2^0 + M_2^r$, followed by a slow decay to M_2^0 . For the MFC procedure (Fig. 4(b)), the sample exhibits a finite magnetization value after cooling down, which is constant in time. After the reduction of the external field to 100 mT at t_3 , the magnetization jumps down to a smaller value $M_3^0 + M_3^r$, followed by an additional slow decrease of magnetization with time to M_3^0 . The jumps most likely correspond to fast relaxation effects, which cannot be resolved due to the finite time (around 100 seconds) required to sweep the external magnetic field.

It is an intrinsic property of glassy systems to react to changes of the magnetic field below its freezing temperature T_f with creeping effects of magnetization.[29] This is caused by the fact that the variation of the field creates a nonequilibrium situation. On the other

hand, if the field is kept constant (FC) during the cooling below T_f , no creeping effects of magnetization are observed. It is important to note that the sketches in Fig. 4 are not to scale. The intensities of the creeping effects, which are denoted with M_1^r , M_2^r and M_3^r in Fig. 4 are generally much smaller than the total magnetization values M_1^0 , M_2^0 and M_3^0 .

Figure 5 (a), (c) and (d) show the magnetization curves $M_1(t)$, $M_2(t)$, and $M_3(t)$ at different temperatures for $\text{Ge}_{0.96}\text{Mn}_{0.04}$, respectively. In Fig. 5(b), $M_1(t)$ is normalized to the magnetization $M_1(t_1)$ immediately after the field was switched on. The strongest relative increase of magnetization is found for $T = 5$ K, whereas for higher and lower temperatures, the relative increase is more moderate.

Many functional forms have been proposed to describe the time dependence of the magnetization in spin glass systems. Reasonable results are obtained in different systems by fitting with logarithmic [7], power law [30], as well as stretched exponential [31] time dependencies. The best fit to our data was obtained by using

$$M_1(t) = M_1^0 - M_1^r \cdot \exp \left[- \left(\frac{t}{\tau} \right)^{1-n} \right], \quad (2)$$

and

$$M_{2/3}(t) = M_{2/3}^0 + M_{2/3}^r \cdot \exp \left[- \left(\frac{t}{\tau} \right)^{1-n} \right], \quad (3)$$

which corresponds to a stretched exponential with an additional constant term M_i^0 . Such a functional form has been used successfully by different other groups to describe relaxation effects in glassy systems.[32, 33, 34] Here, the stretched exponential accounts for the glassy contribution to the magnetization, with τ being a time constant and n affecting the relaxation rate of the glassy component. M_i^r gives the amplitude of the glassy component. The constant term M_i^0 is often interpreted as an intrinsic ferromagnetic contribution to the magnetization, which is assumed to be time independent.[34] The solid lines in Fig. 5 are fitted curves using equations (2) and (3). The parameter n was found to vary between 0.5 and 0.6, except for $M_1(15 \text{ K})$, $M_1(40 \text{ K})$, and $M_3(10 \text{ K})$ which exhibited $n \approx 0.2$. Freitas *et al.*[34] found values of $0.48 < n < 0.6$ for the cluster glass material $\text{La}_{0.7-x}\text{Y}_x\text{Ca}_{0.3}\text{MnO}_3$. Furthermore, for M_1 and M_2 , τ decreases in Fig. 5 from $\tau \approx 6 \times 10^3 \text{ s}$ at 2 K to $\tau \approx 1 \times 10^3 \text{ s}$ at 40 K. For M_3 , τ varies between $1 \times 10^3 \text{ s}$ and $2 \times 10^3 \text{ s}$. Figure 6 shows the temperature dependence of the fit parameters M_0 and M_r . Additionally, the ZFC, FC and MFC $M(T)$

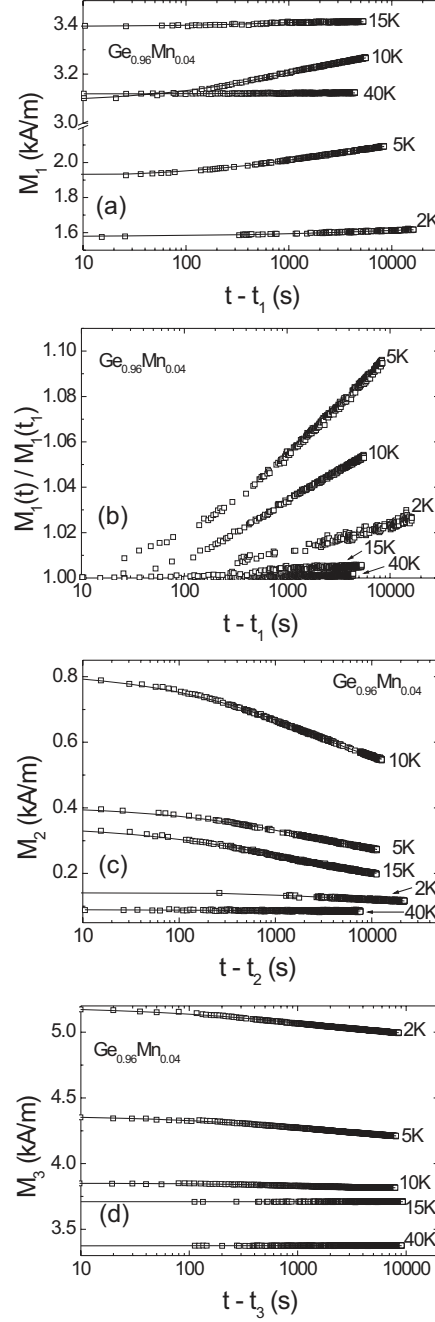


FIG. 5: Increase of magnetization $M_1(t)$ (a) and decay of magnetization $M_2(t)$ (c) and $M_3(t)$ (d) measured as a function of time at different constant measurement temperatures. The solid lines are fitted curves. (b) Magnetization $M_1(t)$ normalized to the magnetization $M_1(t_1)$.

measurements performed at $\mu_0 H_m = 100$ mT (open symbols in Fig. 1) are displayed in the graphs as solid lines.

After switching on the magnetic field at t_1 , the magnetization jumps to $M_1^0 - M_1^r$. Due

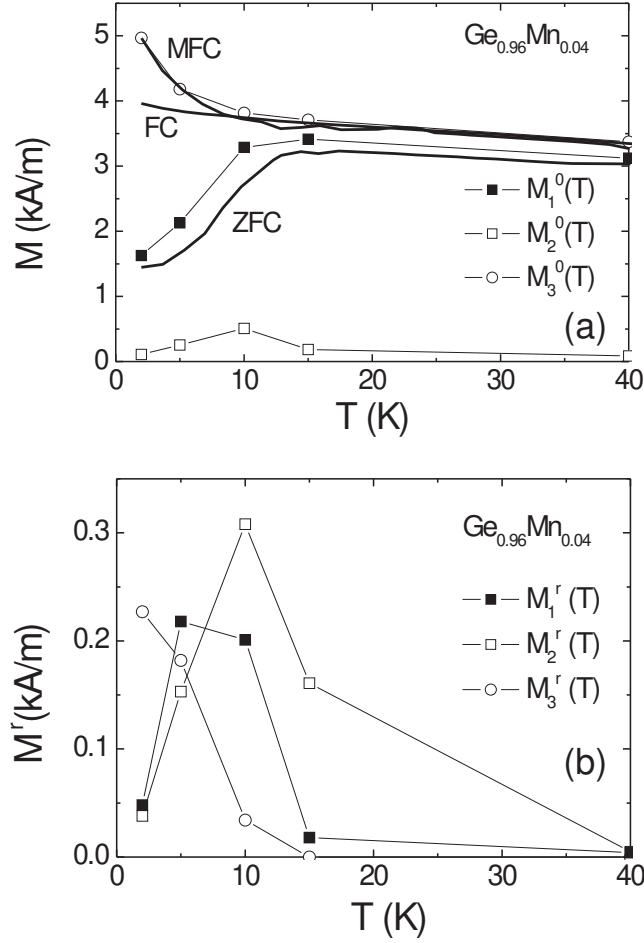


FIG. 6: Temperature dependence of fit parameters (a) M_i^0 and (b) M_i^r of sample $\text{Ge}_{0.96}\text{Mn}_{0.04}$. The solid squares display M_1^0 and M_1^r , the open squares M_2^0 and M_2^r , and the open circles M_3^0 and M_3^r . The thick solid lines in (a) are the ZFC, FC and MFC $M(T)$ measurements performed at $\mu_0 H_m = 100$ mT (open symbols in Fig. 1).

to the additional relaxation effect M_1^r being much smaller than the time-independent M_1^0 (see Fig. 6), the temperature dependence of the magnetization is mainly given by $M_1^0(T)$. $M_1^0(T)$ displayed in Fig. 6(a) by solid squares indeed nicely follows the ZFC magnetization measurement. Therefore, the increase of the ZFC magnetization for increasing temperatures below T_f for the most part has to be an effect of temperature, rather than a relaxation effect in time on the timescale of the $M(T)$ measurement, which takes about 10 minutes from $T = 5$ K to 20 K. The same argument is valid for the decrease at low temperatures in

the MFC measurement: Since M_3^r is much smaller than the time-independent M_3^0 (see Fig. 6), the temperature dependence of the magnetization is mainly given by $M_3^0(T)$, which follows the MFC measurement. Therefore, also the decrease of magnetization in the MFC measurement indeed is a temperature effect.

Furthermore, the temperature dependence of M_2^0 shows a maximum around 10 K (Fig. 6(a)). This kind of measurement, with a switching of the magnetic field from $\mu_0 H = 0$ T to 100 mT and back to 0 T can be interpreted as half a period of a very slow AC experiment with $f \approx 10^{-4}$ Hz. Therefore, the peak in $M_2^0(T)$ is equivalent to a peak in the AC susceptibility and consequently is correlated to a freezing transition in the sample. The peak temperature ≈ 10 K nicely coincides with the freezing temperature $T_f = 12$ K deduced from the difference between the FC and ZFC measurements and $T_{f_0} = 11.8$ K obtained from the Vogel-Fulcher analysis.

Further indications for a freezing transition at low temperatures are obtained from the fit parameters M^r , which denote the magnitude of the relaxation in the sample. Figure 6(b) shows the different $M^r(T)$, with $M_1^r(T)$ and $M_2^r(T)$ exhibiting a peak around $5 \text{ K} \leq T \leq 15 \text{ K}$. This behavior can be rationalized as follows: Coming from higher temperatures, the relaxation components M^r increase as a result of clusters of ferromagnetically coupled magnetic moments in the sample growing in size, whereas for temperatures below T_f , M^r decreases again as a result of cluster freezing. Such peak-like behavior of the relaxation component has already been reported by Freitas *et al.*, [34] who state their material to be a cluster glass. In their publication, the peak in M^r was interpreted as a sign of cluster freezing. A more detailed discussion will be given in Sec. IV.

In summary, also the measurements of the time-dependence of magnetization indicate the presence of a transition to a low temperature frozen state in Ge:Mn, with the transition temperature in complete accordance with the measurements of the temperature-dependence of magnetization and the AC susceptibility presented above.

B. Sample $\text{Ge}_{0.8}\text{Mn}_{0.2}$

The same experiments and analyses were also performed for a $\text{Ge}_{0.8}\text{Mn}_{0.2}$ sample. Figure 7(a) displays the ZFC, FC and MFC curves in $\mu_0 H_m = 1$ mT (solid symbols) and $\mu_0 H_m = 100$ mT (open symbols). Following the method of Li *et al.*, [13] transition tempera-

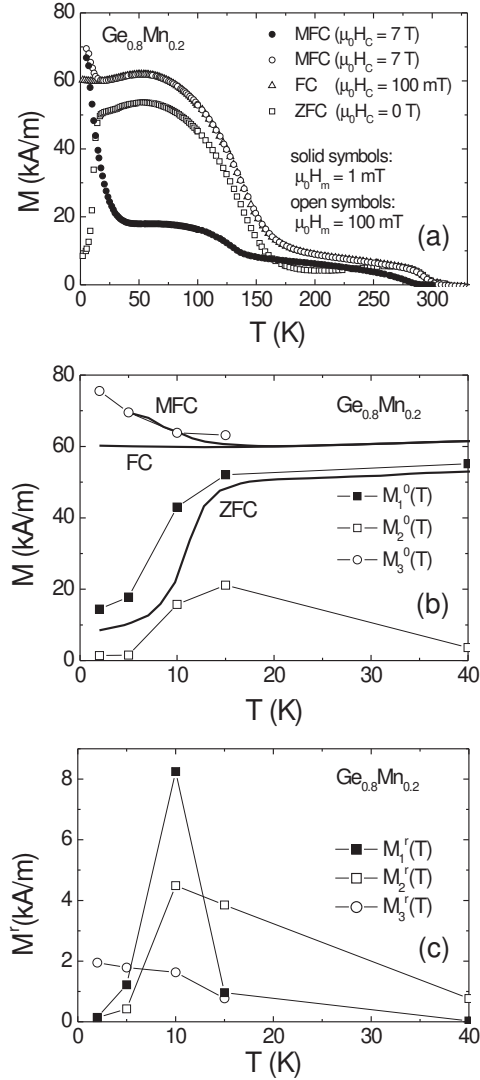


FIG. 7: (a) Temperature dependence of magnetization of sample $\text{Ge}_{0.8}\text{Mn}_{0.2}$. The notation is the same as in Fig. 1. (b) and (c) show the temperature dependence of the fit parameters M^0 and M^r , respectively. The solid squares display M_1^0 and M_1^r , the open squares M_2^0 and M_2^r , and the open circles denote M_3^0 and M_3^r . The thick solid lines in (b) are the ZFC, FC, and MFC $M(T)$ measurements performed at $\mu_0 H_m = 100$ mT, shown by open symbols in (a).

tures of $T_C = 30$ K and $T_C^* = 128$ K were determined for this sample. In contrast to sample $\text{Ge}_{0.96}\text{Mn}_{0.04}$, sample $\text{Ge}_{0.8}\text{Mn}_{0.2}$ shows a pronounced ferromagnetic signal of the Mn_5Ge_3 clusters with $T_C \approx 290$ K even in the measurement with $\mu_0 H_m = 1$ mT. This could be explained by the presence of a thin Mn_5Ge_3 film with an in-plane easy magnetic axis caused

by the shape anisotropy, as already observed by Zeng *et al.*[35] For sample $\text{Ge}_{0.96}\text{Mn}_{0.04}$, the concave shoulder below 200 K could only be observed in the higher external magnetic field $\mu_0 H_m = 100$ mT and therefore was attributed to superparamagnetism above. The fact that for sample $\text{Ge}_{0.8}\text{Mn}_{0.2}$ a weak shoulder can be observed even in the lower magnetic field $\mu_0 H_m = 1$ mT, we attribute to a partial polarization of the superparamagnetic particles by the magnetic field induced by the finite magnetization of the Mn_5Ge_3 precipitates discussed above. For the measurements with $\mu_0 H_m = 100$ mT, the polarization accordingly increases and the shoulder becomes more pronounced.

We want to point out that in spite of the higher abundance of the Mn_5Ge_3 precipitates, the spin-glass like behavior of sample $\text{Ge}_{0.8}\text{Mn}_{0.2}$ is the same as for the sample $\text{Ge}_{0.96}\text{Mn}_{0.04}$ with a lower Mn concentration: We again observe a pronounced difference between the FC and ZFC curves with a freezing temperature $T_f = 15$ K. Measurements of the time dependence of magnetization of this sample qualitatively exhibit the same behavior as already discussed for $\text{Ge}_{0.96}\text{Mn}_{0.04}$. The fit parameters M_1^0 and M_3^0 follow the MFC and ZFC curves and a peak in $M_2^0(T)$ is visible around the freezing temperature (see Fig. 7(b)). Also, the relaxation components $M_1^r(T)$ and $M_3^r(T)$ again show a maximum around 10 K, which is consistent with a freezing transition in the sample at low temperatures (see Fig. 7(c)).

Nevertheless, the AC susceptibility measurements performed on this sample (Fig. 8) indicate a more complicated behavior at higher Mn concentration. For all frequencies, $\chi'(T)$ increases strongly between 20 K and 60 K and subsequently shows a plateau-like behavior up to 115 K with only slightly increasing χ' (Fig. 8(a)). Above this peak temperature, the susceptibility decreases rapidly to $\chi'(T) \approx 0$ above 140 K. The imaginary part of the susceptibility $\chi''(T)$ (Fig. 8(b)) increases monotonically at low temperatures and peaks at $T \approx 110$ K. For higher temperatures, $\chi''(T)$ decreases strongly to $\chi''(T) = 0$ above 125 K.

With increased driving frequencies, both peaks of $\chi'(T)$ and $\chi''(T)$ again shift to higher temperatures with $\Delta T_f' / [T_f' \cdot \Delta \log f] \approx 0.02$ and ≈ 0.03 , respectively. These values are slightly lower than the shift found for the sample $\text{Ge}_{0.96}\text{Mn}_{0.04}$. Furthermore, the peak heights in $\chi'(T)$ and $\chi''(T)$ and the height of the plateau in $\chi'(T)$ decrease for increased driving frequencies.

For $\text{Ge}_{0.8}\text{Mn}_{0.2}$, we observe a good agreement between the $T_f = 15$ K obtained from the FC/ZFC difference and the transition temperature of about 10 K from the measurements of the time dependence of magnetization. However, in the high Mn concentration sample

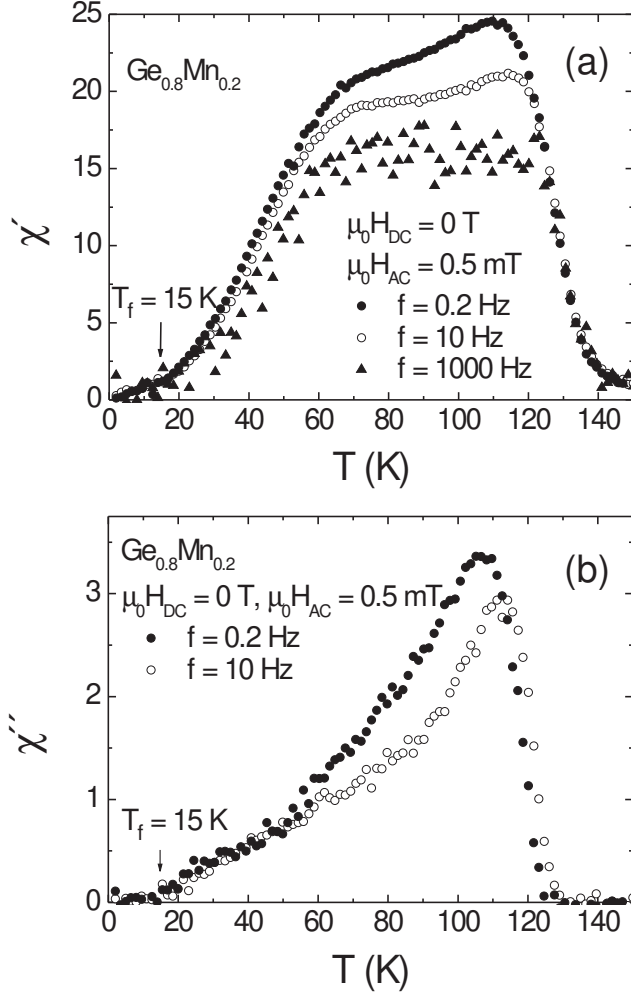


FIG. 8: Real part $\chi'(T)$ (a) and imaginary part $\chi''(T)$ (b) of the AC-susceptibility of $\text{Ge}_{0.8}\text{Mn}_{0.2}$ measured with $\mu_0 H_{DC} = 0$ T and $\mu_0 H_{AC} = 0.5$ mT at $f = 0.2$ Hz (solid circles), $f = 10$ Hz (open circles) and $f = 1000$ Hz (solid triangles).

no peak around T_f is observed in the AC susceptibility measurements, which might be due to the superposition with the more intense plateau-like signal. The peak of sample $\text{Ge}_{0.96}\text{Mn}_{0.04}$ in Fig. 2(a) has an absolute value of $\chi'(T'_f \approx 20 \text{ K}) \approx 0.4$, whereas the plateau-like signal of sample $\text{Ge}_{0.8}\text{Mn}_{0.2}$ in Fig. 8(a) exhibits $\chi'(20 \text{ K}) \approx 2.2$. Consequently, the two samples mainly differ in their AC susceptibility, whereas for both samples we observe a strong difference between zero-field cooled and field cooled magnetization below T_f , as well as relaxation effects of the magnetization after switching the external magnetic field below

T_f .

IV. MICROSCOPIC ORIGIN OF SPIN-GLASS LIKE BEHAVIOR IN Ge:Mn

The experiments discussed above are a strong indication for a transition into a frozen state below T_f . In this section, we discuss possible microscopic origins of the observed glassy behavior.

As mentioned above, the appearance of a concave shoulder in $M(T)$ curves indicates the presence of superparamagnetism in the samples. Li *et al.* explained this behavior in the picture of BMPs.[13] These are formed around T_C^* and grow in size as the temperature is lowered. In the limit of high Mn concentration, Kaminski *et al.* predict that a BMP system undergoes a transition into a randomly ordered state in contrast to a ferromagnetic percolation transition.[36] Indeed, glassy behavior has already been observed experimentally in Te compensated $\text{Ga}_{0.915}\text{Mn}_{0.085}\text{As}$. [8] However, it is questionable, whether $\text{Ge}_{0.96}\text{Mn}_{0.04}$ can be described within the high Mn concentration limit of Ref. [36]. The interpretation of the magnetization data by an onset of local ferromagnetism below a first transition temperature and the transition to a frozen, glassy state at a lower temperature due to cluster freezing is similar to the scenario reported for a so-called cluster glass material. A cluster glass consists of ferromagnetic clusters, which grow in size with decreasing temperature down to a temperature, at which they freeze due to intercluster frustration.[34] Like in the model of BMPs, at first local ferromagnetism occurs (the formation of ferromagnetic clusters in the cluster glass on the one hand and the formation of BMPs in the BMP model for DMSs on the other hand). These local ferromagnetic regions both grow in size, finally leading to a disordered glassy state at low temperatures.

In cluster glass materials, a two-peak structure in the susceptibility measurements was observed.[34] The peak in the susceptibility occurring at the higher temperature was assigned to be an indication for the formation of ferromagnetic clusters, whereas the low temperature peak was attributed to cluster freezing in the sample.[34] The temperature of the AC susceptibility peak of $\text{Ge}_{0.8}\text{Mn}_{0.2}$ (≈ 115 K) is indeed close to the value of $T_C^* = 128$ K, determined from the temperature below which the formation of BMPs is supposed to set in following Li *et al.* Therefore, in analogy to the cluster glass described above, the peak around ≈ 115 K in the AC susceptibility might be connected to the onset of local ferromagnetism due to the

formation of BMPs. However, the position of the high temperature peak observed by Freitas *et al.*, [34] which is thought to correspond to the local onset of ferromagnetism within the clusters, was found to be independent of frequency in contrast to the weak frequency dependence detected here. Furthermore, no second high temperature peak could be observed for $\text{Ge}_{0.96}\text{Mn}_{0.04}$. Therefore, the AC behavior exhibited by the Ge:Mn samples studied here is not completely identical to that reported for $\text{La}_{0.7-x}\text{Y}_x\text{Ca}_{0.3}\text{MnO}_3$ in Ref. [34].

The superparamagnetic response in the temperature range between 20 K and 200 K might also be explained by regions with locally increased Mn concentration, as already proposed theoretically for GaMnAs by Timm *et al.* [37] Within these regions, the holes could be regarded as delocalized leading to ferromagnetic coupling at sufficiently low temperatures (below T_C^*). [18] Indeed, Park *et al.* [9] observed Mn rich ($x \approx 0.10 - 0.15$) nanoclusters via transmission electron microscopy. Li *et al.* conjecture that such physical clusters could be viewed as a generalization of BMPs. [14] Assuming that these nanoclusters are embedded in a more diluted Mn-doped Ge matrix exhibiting a transition into a spin glass state below T_f , a freezing of the clusters with random orientation below T_f would be expected [24].

Alternatively, the freezing transition might also occur inside the nanoparticles themselves. For $\text{Ge}_{1-x}\text{Mn}_x$, Zhao *et al.* [38] proposed an oscillatory exchange constant explicitly following the Ruderman-Kittel-Kasuya-Yosida (RKKY) formula. Assuming a high charge carrier concentration in the nanoclusters, this could lead to the competing interactions between the localized Mn spins inside the clusters required to form a spin glass state.

Finally, we would like to remark that the spin glass-like phase can be observed irrespective of the presence of Mn_5Ge_3 clusters in the samples. Samples free of Mn_5Ge_3 clusters also exhibit the effects typical for spin glasses reported in this work. [39]

V. CONCLUSION

We have extensively studied the magnetic properties of $\text{Ge}_{1-x}\text{Mn}_x$ with a focus on the low temperature state using three different methods spanning seven orders of magnitude in time scales. Instead of a ferromagnetic percolation transition, [13, 14] we clearly find a glassy state below $T_f \approx 15$ K in samples both with a low and a high Mn concentration. For both samples, we observe a strong difference between the zero-field cooled and field cooled magnetization below T_f , as well as relaxation effects of the magnetization after switching the external

magnetic field below T_f . In addition, AC susceptibility measurements on $\text{Ge}_{0.96}\text{Mn}_{0.04}$ show a peak around T_f , with the peak position T'_f shifting as a function of the driving frequency f by $\Delta T'_f/[T'_f \cdot \Delta \log f] \approx 0.06$. These findings consistently show that Ge:Mn exhibits spin-glass like magnetic behavior at low temperatures, and that this dilute magnetic semiconductor cannot be regarded as a conventional ferromagnet.

Acknowledgments

Our work was supported by Deutsche Forschungsgemeinschaft through SFB 631. Discussions with Stefan Ahlers, Dominique Bougeard, and Martin Stutzmann are gratefully acknowledged.

-
- [1] K. W. Edmonds, P. Boguslawski, K. Y. Wang, R. P. Campion, S. N. Novikov, N. R. S. Farley, B. L. Gallagher, C. T. Foxon, M. Sawicki, T. Dietl, M.B. Nardelli, J. Bernholc, Phys. Rev. Lett. **92**, 037201 (2004).
 - [2] A.M. Nazmul, S. Sugahara, and M. Tanaka, Phys. Rev. B **67**, 241308(R) (2003).
 - [3] D. Chiba, K. Takamura, F. Matsukura, and H. Ohno, Appl. Phys. Lett. **82**, 3020 (2003).
 - [4] S. P. McAlister, J. K. Furdyna, and W. Giriat, Phys. Rev. B **29**, 1310 (1984).
 - [5] R. R. Galazka, S. Nagata, and P. H. Keesom, Phys. Rev. B **22**, 3344 (1980).
 - [6] S. B. Oseroff, Phys. Rev. B **25**, 6584 (1982).
 - [7] S. Dhar, O. Brandt, A. Trampert, K. J. Friedland, Y. J. Sun, and K. H. Ploog, Phys. Rev. B **67**, 165205 (2003).
 - [8] S. U. Yuldashev, H. C. Jeon, H. S. Im, T. W. Kang, S. H. Lee, and J. K. Furdyna, Phys. Rev. B **70**, 193203 (2004).
 - [9] Y. D. Park, A. T. Hanbicki, S. C. Erwin, C. S. Hellberg, J. M. Sullivan, J. E. Mattson, T. F. Ambrose, A. Wilson, G. Spanos, and B. T. Jonker, Science **295**, 651 (2002).
 - [10] S. Cho, S. Choi, S. C. Hong, Y. Kim, J. B. Ketterson, B.-J. Kim, Y. C. Kim, and J.-H. Jung, Phys. Rev. B **66**, 033303 (2002).
 - [11] N. Yamada, K. Maeda, Y. Usami, and T. Ohoyama, J. Phys. Soc. Jpn. **55**, 3721 (1986).

- [12] J.-S. Kang, G. Kim, S. C. Wi, S. S. Lee, S. Choi, S. Cho, S. W. Han, K. H. Kim, H. J. Song, H. J. Shin, A. Sekiyama, S. Kasai, S. Suga, B. I. Min, Phys. Rev. Lett. **94**, 147202 (2005).
- [13] A. P. Li, J. Shen, J. R. Thompson, and H. H. Weitering, Appl. Phys. Lett. **86**, 152507 (2005).
- [14] A. P. Li, J. F. Wendelken, J. Shen, L. C. Feldman, J. R. Thompson, and H. H. Weitering, Phys. Rev. B **72**, 195205 (2005).
- [15] N. Yamada, J. Phys. Soc. Jpn. **59**, 273 (1990).
- [16] C. Bihler, C. Jaeger, T. Vallaitis, M. Gjukic, M. S. Brandt, E. Pippel, J. Woltersdorf, and U. Gösele, Appl. Phys. Lett. **88**, 112506 (2006).
- [17] A. Kaminski and S. Das Sarma, Phys. Rev. Lett. **88**, 247202 (2002).
- [18] A. Kaminski and S. Das Sarma, Phys. Rev. B **68**, 235210 (2003).
- [19] J. K. Furdyna, J. Appl. Phys. **64**, R29 (1988).
- [20] J. M. De Teresa, M. R. Ibarra, J. Garcia, J. Blasco, C. Ritter, P. A. Algarabel, C. Marquina, and A. del Moral, Phys. Rev. Lett. **76**, 3392 (1996).
- [21] C. A. Cardoso, F. M. Araujo-Moreira, V. P. S. Awana, E. Takayama-Muromachi, O. F. de Lima, H. Yamauchi, and M. Karppinen, Physica C **408**, 183 (2004).
- [22] S. Geschwind, A. T. Ogielski, G. Devlin, J. Hegarty, and P. Bridenbaugh, J. Appl. Phys. **63**, 3291 (1988).
- [23] A. Mauger, J. Ferre, M. Ayadi, and P. Nordblad, Phys. Rev. B **37**, 9022 (1988).
- [24] J. A. Mydosh, *Spin Glasses - An experimental introduction* (Taylor & Francis, London, 1993).
- [25] J. L. Tholence, Solid State Commun. **35**, 113 (1980).
- [26] S. Shtrikman and E. P. Wohlforth, Phys. Lett. A **85**, 467 (1981).
- [27] M. Koyano, M. Suezawa, H. Watanabe, and M. Inoue, J. Phys. Soc. Jap. **63**, 1114 (1993).
- [28] R. N. Bhowmik and R. Ranganathan, J. Appl. Phys. **93**, 2780 (2003).
- [29] R. Rammel and J. Souletie, *Magnetism of Metals and Alloys* (North-Holland, New York, 1982).
- [30] W. Kinzel, Phys. Rev. B **19**, 4595 (1979).
- [31] G. C. DeFotis, G. S. Coker, J. W. Jones, C. S. Branch, H. A. King, J. S. Bergman, S. Lee, and J. R. Goodey, Phys. Rev. B **58**, 12178 (1998).
- [32] P. Mitchler, R. M. Roshko, and W. Ruan, J. Appl. Phys. **73**, 5460 (1993).
- [33] A. Maignan, A. Sundaresan, U. V. Varadaraju, and B. Raveau, J. Magn. Magn. Mat. **184**, 83 (1998).

- [34] R. S. Freitas, L. Ghivelder, F. Damay, F. Dias, and L. F. Cohen, Phys. Rev. B **64**, 144404 (2001).
- [35] C. Zeng, S. C. Erwin, L. C. Feldman, A. P. Li, R. Jin, Y. Song, J. R. Thompson, and H. H. Weitering, Appl. Phys. Lett. **83**, 5002 (2003).
- [36] A. Kaminski, V. M. Galitski, and S. Das Sarma, Phys. Rev. B **70**, 115216 (2004).
- [37] C. Timm, F. Schäfer, and F. von Oppen, Phys. Rev. Lett. **89**, 137201 (2002).
- [38] Y. J. Zhao, T. Shishidou, and A. J. Freeman, Phys. Rev. Lett. **90**, 047204 (2003).
- [39] S. Ahlers (private communication).